

# Discovery and analysis of Gamma Doradus type pulsations in the F0 IV star HR 2740 $\equiv$ QW Pup

E. Poretti<sup>1</sup>, C. Koen<sup>2</sup>, P. Martinez<sup>2</sup>, F. Breuer<sup>3</sup>, D. de Alwis<sup>3,4</sup>, H. Haupt<sup>3</sup>

<sup>1</sup>*Osservatorio Astronomico di Brera, Via Bianchi 46, I-22055 Merate, Italy*

<sup>2</sup>*South African Astronomical Observatory, PO Box 9, Observatory 7935, Cape, South Africa*

<sup>3</sup>*Summer Student at the South African Astronomical Observatory*

<sup>4</sup>*Arthur C. Clarke Centre for Modern Technologies, Moratuwa, Sri Lanka*

## ABSTRACT

We present multi-site photometric observations of the F0 IV star HR 2740 $\equiv$ QW Pup which reveal it to be a  $\gamma$  Dor type variable pulsating with four frequencies: 1.0434, 0.9951, 1.1088, 0.9019 d $^{-1}$ . These data were obtained at the European Southern Observatory and South African Astronomical Observatory over a time baseline spanning from 1997 January 14 to 1997 February 11. The 1.0434 d $^{-1}$  term dominates in amplitude (10 mmag) over the other three (each less than 5 mmag); the light curve comprising these four frequencies seems to be very stable and no residual power is left in the power spectrum. During the analysis particular attention was paid to methodological aspects, which cannot be neglected considering the proximity of the frequencies to 1 d $^{-1}$ .

Physical parameters were also derived for all the well-known  $\gamma$  Dor stars, confirming that this class is very homogenous. In the framework of the campaign, two Ap stars (OU Pup $\equiv$ HR 2746 and PR Pup $\equiv$ HR 2761) were also observed. The photometric differences between these rotating variables and HR 2740 are emphasized, corroborating the pulsational nature of the  $\gamma$  Dor stars. It is further demonstrated that the rotational splitting cannot be a suitable explanation of the observed frequency content of HR 2740.

**Key words:** Stars: individual: HR 2740 – Stars: individual: OU Pup – Stars: individual: PR Pup – Stars: pulsation – Methods: data analysis

## 1 INTRODUCTION

The number of variable stars located at or near the cool border of the classical instability strip has rapidly increased in the recent years; they show complex light curves, generated by the superposition of many periods, ranging from a few hours to a few days. Balona et al. (1994) supplied observational evidence that  $\gamma$  Doradus is a pulsating variable. Poretti et al. (1996; a more detailed paper is in preparation) found a large spread in the frequencies observed in the light curve of HD 224945, corroborating the pulsational hypothesis. The existence of a new class of pulsating variable stars of around spectral type F0, that is redward of the cool border of the classical instability strip, is now accepted and  $\gamma$  Doradus has been designated the prototype of this class. These stars have periods on order of 1 d and  $V$  amplitudes  $\sim$ 0.02 mag.

Since  $\gamma$  Doradus stars are located in a region of the HR diagram where variable stars are not expected, they were often used as comparison stars; a revisit of old photometric measurements was undertaken in order to detect new

members. In such a way, Breger et al. (1997) suggested that the low frequency content of the light variability of the  $\delta$  Sct star 4 CVn must be ascribed to its comparison star, the F0 star HD 108100.

The light variability of the F0 IV star HR2740 $\equiv$ HD 55892 $\equiv$ QW Pup was discovered by Hensberge et al. (1981), who used it as a comparison to measure some Ap stars. On the basis of 20  $uvby$  data collected on 16 nights spanning 41 days, they derived a period of  $0.9363 \pm 0.005$  d and considered HR 2740 as a “mild Ap star”. However, Hensberge et al. also emphasized the lack of the continuum depression near 520 nm (typical for Ap stars) and the necessity to perform additional photometry to confirm period and classification.

The link between HR 2740 and the  $\gamma$  Doradus stars was definitely established when we took some high resolution spectra of HR 2740 (considered by Slettebak et al. 1975 as standard for rotational velocity) and clearly detected some line profile variations. Now that many F0 stars are known to be variable and are grouped into a new class, it is quite obvious to realize that Hensberge et al.

(1981) performed a pre-discovery observation of a  $\gamma$  Dor variable star.

## 2 PHOTOMETRIC OBSERVATIONS

As demonstrated by the previous experiences on other  $\gamma$  Dor stars, single-site observations are not suitable to study their light variability. The aliases at  $\pm 1\text{d}^{-1}$  are strong, multiperiodicity is commonly observed and the signal is concentrated near  $1\text{ d}^{-1}$ : all these factors produce complex spectral patterns, where the detection of the true frequencies is a difficult exercise (see for example Mantegazza et al. 1994). For these reasons, new observations of HR 2740 were obtained from two sites: at La Silla (European Southern Observatory, Chile) and Sutherland (South African Astronomical Observatory, South Africa). Unfortunately a third observing site located in New Zealand could not join the project.

Moreover, it was decided to add the Ap stars HR 2761 $\equiv$ PR Pup and HR 2746 $\equiv$ OU Pup to the observing programme: these variables are known to have periods similar in length to that expected for HR 2740, a small amplitude and well defined light curve. Located near HR 2740, PR and OU Pup provide an excellent litmus-paper to compare and check the results obtained on HR 2740. HR 2762 and HR 2789 were selected as comparison stars; since all the stars are bright, the Strömgren filters were preferred to the Johnson ones.

The 50-cm telescope equipped with a EMI 9789QA tube was used at ESO (observer E. Poretti). The measurements were performed on eight consecutive nights, from 1997 January 29–30 to 1997 February 5–6. The frequency of measures was different for the different stars: since the variability of the two Ap stars was known to be slow and monoperiodic, HR 2740 was measured (in *uvby*) 6 times more frequently.

A 50-cm telescope equipped with a Hamamatsu tube was also used at SAAO; however, to avoid saturation effects the telescope was stopped out at an aperture of 28 cm. A first string of data covers 6 nights of 7 from 1997 January 14–15 to 20–21 (observers P. Martinez, D. de Alwis, F. Breuer, H. Haupt); then a second string of data covers 10 nights from 1997 January 28–29 to 1997 February 10–11 (observers C. Koen and P. Martinez). Measurements were performed in *b* and *y* light and the two Ap stars were measured more frequently than at ESO.

## 3 DATA REDUCTION

### 3.1 Differential photometry

The data reduction was performed following the method described by Poretti & Zerbi (1993), which allows us to determine the behaviour of the extinction coefficient  $k_\lambda(t)$  during the night. Table 1 summarizes the results of the behaviour of  $k_\lambda$ .

Since the measurements were generally performed in excellent photometric conditions, the very small fluctuations observed in the  $k_\lambda(t)$  values (upper part of Tab. 1) and the close proximity of all the stars did not introduce any appreciable change (a very few measurements changed by 1 or 2 mmag) with respect to the magnitude differences calculated by the usual Bouguer's line (i.e.  $k_\lambda$  considered as

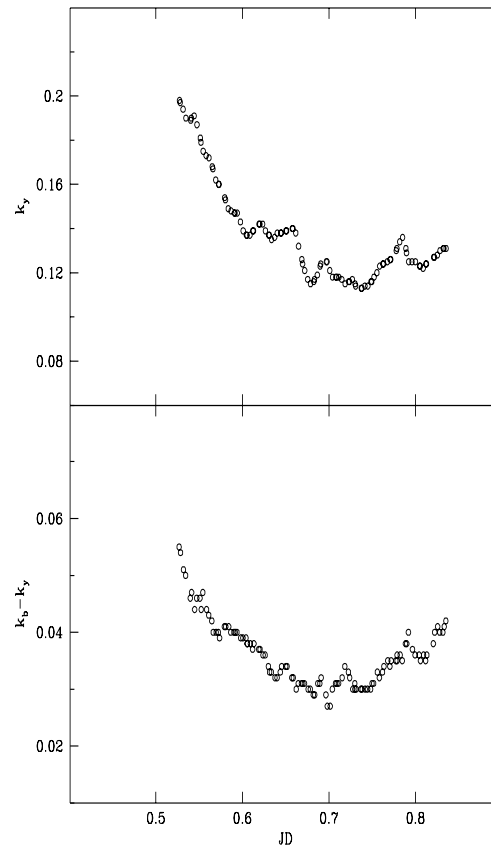


**Figure 1.** The variability of the extinction coefficient on night JD 2450480 as observed at ESO; the behaviour depends on the wavelength, as showed by the differences between the  $k_b$  and  $k_y$  values

**Table 1.** Extremum values for the extinction coefficient. Units are mag airmass $^{-1}$

Filter	ESO		SAAO	
	Min–Max		Min–Max	
All the nights				
<i>u</i>	0.49–0.70		–	
<i>v</i>	0.27–0.44		–	
<i>b</i>	0.11–0.26		0.14–0.21	
<i>y</i>	0.09–0.20		0.09–0.15	
Maximum range in one night				
<i>u</i>	0.52–0.70		–	
<i>v</i>	0.30–0.44		–	
<i>b</i>	0.14–0.25		0.16–0.20	
<i>y</i>	0.11–0.20		0.10–0.15	
	JD 2450480		JD 2450490	

a constant value). In turn, this comparison confirms the stability of a photon counting system properly controlled (i.e. no instrumental drift from one night to the next) and the colour-dependant variation of the extinction coefficient (lower part of Tab. 1) strongly supports the atmospheric origin of the variation. Changes in transparency were occasionally observed when the sky became clear after a period of cloudy weather (see lower part of Tab. 1 and Fig. 1)

For sake of homogeneity, the same algorithm was used both for ESO and SAAO measurements to calculate the differential magnitudes of all the stars respect with HR 2762. No variability was found in the light curves of HR 2789, i.e. both the comparison stars can be considered constant in brightness. As regards the 370 ESO measurements, the rms residuals are 3.9, 3.2, 3.3 and 3.5 mmag in the *uvby* colours, respectively; as regards the 265 SAAO measurements they are 3.1 and 2.9 mmag in the *by* colours, respectively. After alignment of the mean magnitudes, the resulting residual rms's are 3.2 and 3.3 mmag in the *by* colours, respectively.

### 3.2 Mean magnitudes alignments

The determination of the systematic difference in the zeropoints constitutes a serious problem when dealing with multiperiodicities near 1 d and different instrumental systems. Let us discuss the matter starting from the differential measurements of the two Ap stars, which are monoperiodic variables (see also the next section). In this case, once the period is determined by analyzing each dataset, it is possible to obtain the two zeropoints simply by performing a least-squares fit.

In the case of OU Pup, the SAAO and ESO datasets each have very good phase coverage and they can be used separately to yield two sets of parameters; it was then possible to verify that amplitudes and phases agreed very well and the difference between the two zeropoints immediately yielded the systematic shift in magnitude. In the case of PR Pup, only the SAAO dataset covers in phase the whole light curve; therefore a different procedure was followed. From the fit of SAAO data we calculated the frequency and amplitude of the sine-wave and then we fitted the ESO data by keeping these values locked. In this way we avoided obtaining unreliable values for the amplitude, since the extrema of the light curve not well covered in the ESO data. From this locked fit the ESO zeropoint was also derived and the two datasets could be merged.

The case of HR 2740 is quite different. As described above, multisite observations are necessary to decipher the light curve and hence no preliminary solution can be reliably used. The same problem was recently discussed by Breger et al. (1997; see their Sect. 2); those authors decided to subtract mean values from each dataset and then merge the data. This procedure is particularly dangerous in the case of  $\gamma$  Dor stars since most of the signal is concentrated near 1 d<sup>-1</sup> and then and a considerable reduction in amplitude can occur. This can be easily verified in the case of OU Pup, where the light curves over the period 0.918 d were obtained separately for each dataset: the shifts so calculated are 1.8 and 2.1 mmag in *b* and *y* light; on the other hand, the mean magnitudes are shifted by 4.1 and 3.9 mmag, respectively.

Therefore we decided to calculate the systematic shifts between the two datasets by using the overlapping segments of the light curve; the end of the observations at Sutherland coincides with the start at La Silla. As noted by Breger et al. (1997), measures done at large airmasses are not very accurate. However this method can provide satisfactory results; for example, starting from an error of about 3 mmag on a single observation (as in our case) and admitting that this error may be doubled at large airmass, if we have 4 measurements for each site performed in the overlap time, then

in one night the systematic shift can be calculated with a precision of about 4.2 mmag and 5 nights are sufficient to reduce the error on the shift to less than 2.0 mmag. Of course, it is sufficient to have 9 nights or 8 measurements per site to ensure an error of about 1 mmag. So, the potential of the overlap method should be carefully considered in the planning and in the data reduction of multisite campaigns. In the case of HR 2740, we applied this method and determined a systematic shift of 13 mmag in *b* light and 6 mmag in *y* light; these values are slightly different from those obtained by aligning the arithmetic average of the two datasets (17 and 10 mmag, respectively). From a close inspection of the light curves it seems that the alignments produced by the values supplied by the average method are not satisfactory; we will discuss this point again at the end of next section.

## 4 THE FREQUENCY ANALYSIS

To perform the frequency analysis we used the Vaniček's (1971) least-squares technique, which searches for multiple periods without relying on prewhitening, thus avoiding dangerous deformations in the power distribution. The 'reduction factor'  $RF = 1 - \sigma_{fin}^2 / \sigma_{in}^2$  is calculated for each trial frequency.  $\sigma_{in}^2$  is the variance before considering it and  $\sigma_{fin}^2$  is the variance after considering it; if the RF is close to 1 it means that the frequency fits the data very well, greatly reducing the variance, while if RF is near 0 this means that the frequency doesn't fit the data appreciably.

The parameters of the least-squares fit were calculated by fitting the data to the series

$$\Delta m(t) = \Delta m_0 + \sum_{j=1}^M A_j \cos[2\pi f_j(t - T_0) + \phi_j] \quad (1)$$

### 4.1 OU Pup

The frequency analysis of the ESO and SAAO measurements were performed separately. Both yielded 1.09 d<sup>-1</sup> as the highest peak in the power spectrum; introducing it as the "known constituent" (k.c.) the 2*f* harmonic was detected. These two terms strongly reduced the variance and no further frequency components could be detected. The measurements were merged by means of the procedure described above. We confirm the period value given by Heck et al. (1987), i.e. 0.9189 d; the mean light curves are shown in Fig. 2 and are characterized by a constant brightness for about 0.35% of the period. The simplest explanation of such a variability is to think of a bright feature on the stellar surface carried through the visible disk by rotation; this feature is not always seen from the Earth and its disappearance produces the standstill at minimum brightness. As can be noted (see Fig. 2 and Tab. 2), the *u* light curve has an amplitude much larger than in the other colours; in particular, in *y* light the curve is very shallow.

### 4.2 PR Pup

The frequency analysis supplied only one peak at 0.485 d<sup>-1</sup> and no harmonic. This value for the frequency is particularly unfavourable and hampered any direct calculation of

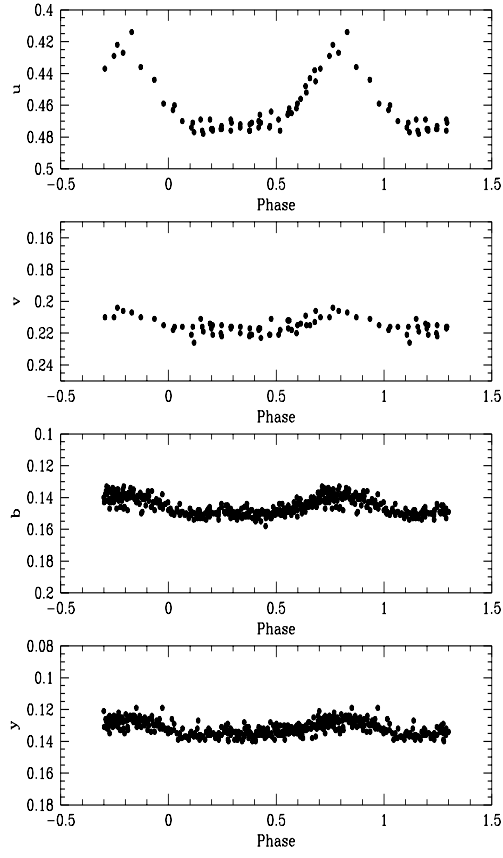


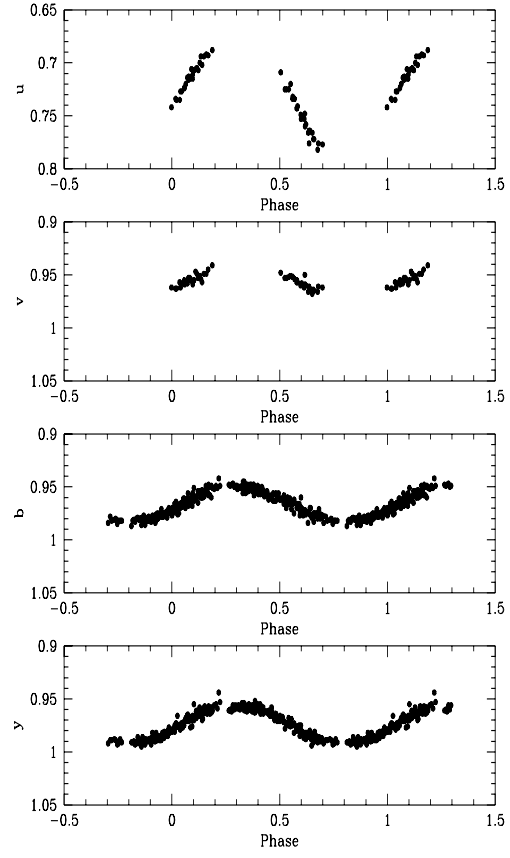
**Figure 2.** *uvby* light curves of OU Pup. *b* and *y* measurements were performed both at ESO and SAAO, while *u* and *v* data were obtained only at ESO

reliable  $A_0$  values. However, the procedure described in the previous section allowed us to obtain the mean light curves shown in Fig. 3. In the case of PR Pup the light curve is perfectly sinusoidal, implying that the feature responsible for the variability is always visible from the Earth; also in this case the largest amplitude is observed in *u* light.

There is a bit of confusion about the period of this star in the literature: Heck et al. (1987) report 1.9346 d (i.e.  $0.517 \text{ d}^{-1}$ ), Catalano & Leone (1993) report 2.06370 d (i.e.  $0.485 \text{ d}^{-1}$ ). It is evident that one period is the alias of the other; our double-site observations allowed us to exclude the former and to confirm the latter. We determined a time of minimum brightness at HJD 2450464.59, with an O-C of  $-0.47$  d respect with the ephemeris reported by Catalano & Leone (1993). If we admit no period variation and no phase shift, a refined period of 2.063243 d can be derived by combining the two times of minimum light. The parameters of the least-squares fit are reported in Tab. 2.

### 4.3 HR 2740

Figure 4 shows the light curve in *b*; in the intervals JD 2450463–2450470 and JD 2450486–2450491 we have only measurements carried out at SAAO (upper and lower panel), while in the interval JD 2450477–2450486 we have contiguous measurements carried out at SAAO and ESO (middle panel).

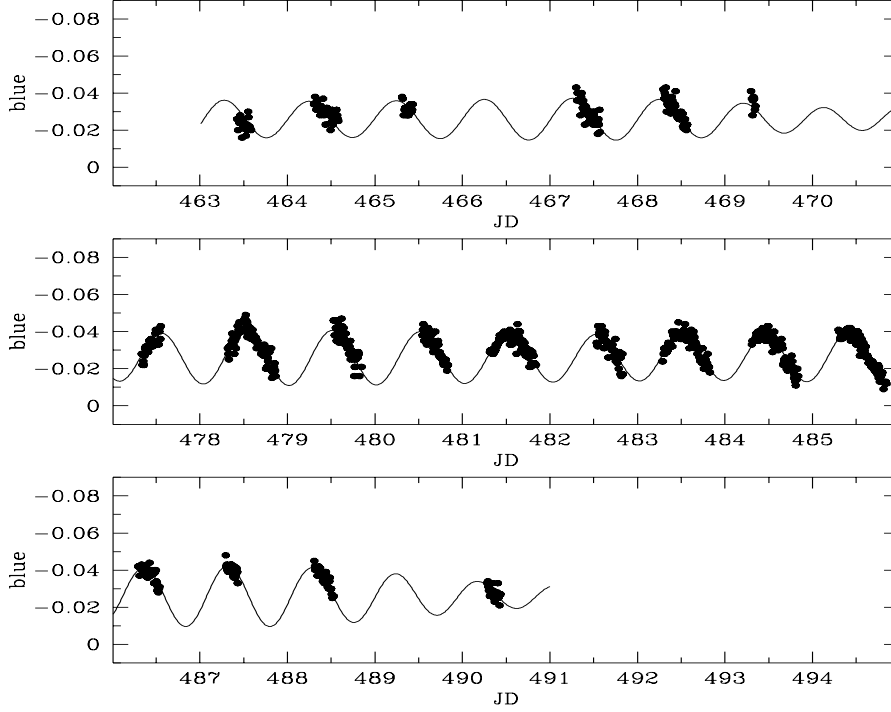


**Figure 3.** *uvby* light curves of PR Pup. The unsatisfactory phase coverage of the single-site measurements is shown by the *u* and *v* light curves (ESO only); while *b* and *y* measurements were performed both at ESO and SAAO

Both *b* and *y* data were analyzed in frequency and we discuss here the former, since in that colour the amplitudes are larger. A simple look at the middle panel of Fig. 4 clearly suggests a period close to 1 day and a regular light curve. The ESO measurements always show a regular decrease in magnitude, perfectly linked to the SAAO ones which end at maximum brightness. However, the SAAO light curve at the beginning of the campaign is less regular and does not seem to repeat itself regularly from one night to the next. We firstly considered the dataset comprising the measurements obtained from JD 2450477 to JD 2450486 only, since the spectral window of this dataset is relatively free from the  $1 \text{ d}^{-1}$  alias and this allows more reliable frequency identifications. Indeed we obtained a well defined peak at  $f_1=1.02 \text{ d}^{-1}$ , explaining the variation evidenced in the middle panel of Fig. 4. To proceed further, we included it as a known constituent (k.c.) in the successive least-squares search; this means that considering Eq. (1) applied to *b* data, the unknowns in the second search were  $\Delta b_0, A_1, \phi_1, f_2, A_2, \phi_2$ , while the  $f_1=1.02 \text{ d}^{-1}$  value was kept fixed. As a second peak we found  $f_2=0.90 \text{ d}^{-1}$ ; the fit with  $f_1$  and  $f_2$  leaves a residual rms of 3.1 mmag and considering that this value is very close to the standard deviation of the measurements of HR 2762 we could conclude that these two frequencies yield a good explanation of the observed light curve; only small residual peaks are visible in the spectrum obtained by

**Table 2.** Least-squares fit of the data on PR Pup and OU Pup

Star	<i>u</i>		<i>v</i>		<i>b</i>		<i>y</i>	
	Ampl. [mmag]	Phase [rad]	Ampl. [mmag]	Phase [rad]	Ampl. [mmag]	Phase [rad]	Ampl. [mmag]	Phase [rad]
OU Pup	23.5	4.43	5.2	4.41	5.4	4.36	4.0	4.31
$f=1.0889 \text{ d}^{-1}$	$\pm 5.2$	$\pm 0.54$	$\pm 0.7$	$\pm 0.13$	$\pm 0.4$	$\pm 0.12$	$\pm 0.4$	$\pm 0.14$
$2f$	9.4	5.58	2.4	5.93	2.1	5.69	1.7	5.07
	$\pm 5.5$	$\pm 0.59$	$\pm 0.7$	$\pm 0.26$	$\pm 0.5$	$\pm 0.26$	$\pm 0.4$	$\pm 0.33$
$T_0 = \text{Hel. J.D. } 2450463.000$								
$\Delta m_0$	$0.4575 \pm 0.0006$		$0.2148 \pm 0.0005$		$0.1465 \pm 0.0002$		$0.1325 \pm 0.0002$	
Residual rms	3.7 mmag		3.2 mmag		2.9 mmag		2.9 mmag	
PR Pup	56.6	1.60	14.8	1.37	16.2	1.38	17.6	1.43
$f=0.4846 \text{ d}^{-1}$	$\pm 4.4$	$\pm 0.14$	$\pm 1.6$	$\pm 0.32$	$\pm 0.3$	$\pm 0.05$	$\pm 0.3$	$\pm 0.05$
$T_0 = \text{Hel. J.D. } 2450463.000$								
$\Delta m_0$	$0.7292 \pm 0.0007$		$0.9558 \pm 0.0004$		$0.9663 \pm 0.0002$		$0.9740 \pm 0.0002$	
Residual rms	4.8 mmag		3.0 mmag		3.2 mmag		3.1 mmag	

**Figure 4.** *b* light curves of HR 2740.

introducing  $f_1$  and  $f_2$  as k.c. It must be emphasized that the power spectra are absolutely flat after  $4 \text{ d}^{-1}$ ; the signal is entirely contained in the low frequency range.

On the basis of the above analysis, the light variation of HR 2740 seems to be well described by one dominant frequency and one or two low-amplitude terms. However, the analysis of the measurements performed at SAAO in the in-

terval between JD 2450463 and 2450470 disrupted this simple scenario. When considering the solution just obtained, we were not able to fit this part of the light curve in a satisfactory way. Since the rising branch was observed in the JD 2450478–2450487 interval and the gap was only 8 days, the phases on the  $f_1 = 1.02 \text{ d}^{-1}$  cycle should be the only slightly (less than 0.2 period) shifted towards the minimum

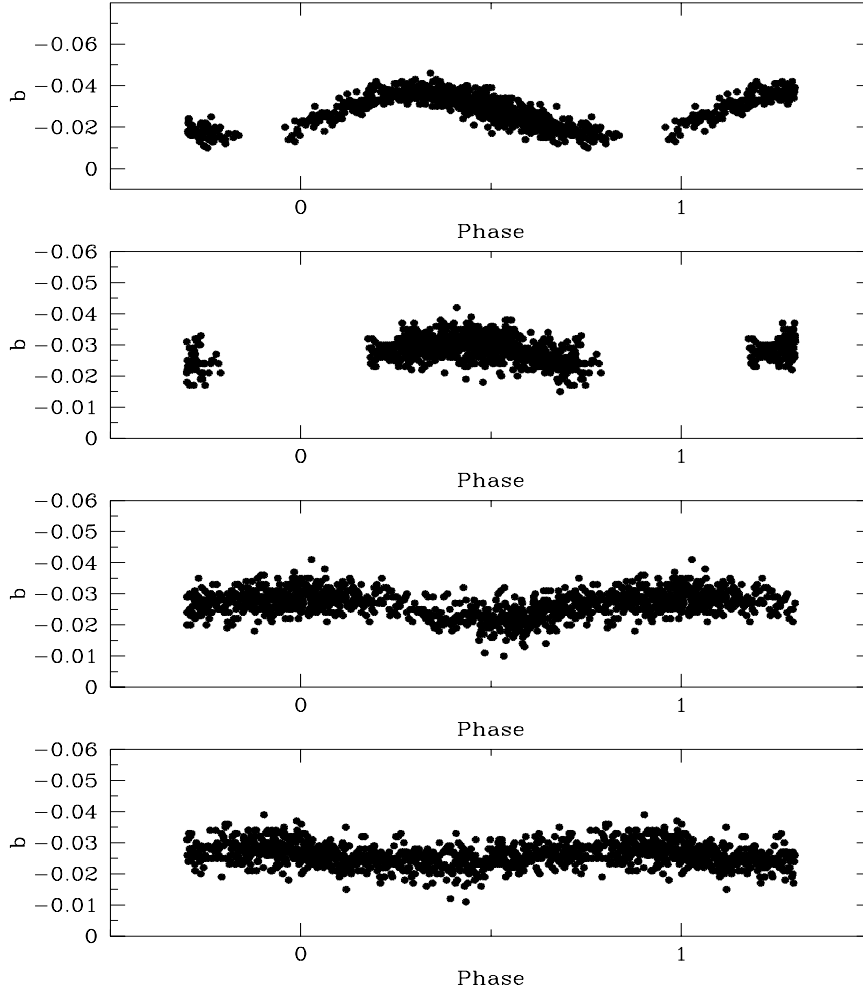


**Figure 5.** Power spectra of the  $b$  light curves of HR 2740. From top to bottom: with no known constituent (k.c.), with  $f_1=1.04 \text{ d}^{-1}$  as k.c.; with  $f_1$  and  $f_2=1.10 \text{ d}^{-1}$  as k.c.'s; with  $f_1, f_2, f_3=0.90 \text{ d}^{-1}$  as k.c.'s; with  $f_1, f_2, f_3, f_4=0.995 \text{ d}^{-1}$  as k.c.'s

light branch in the JD 2450463–2450470 interval, but this was not observed. Also the measurements carried out in the JD 2450486–2450491 interval could not be fitted in a satisfactory way; in particular, the descending branch observed in the last night at SAAO is too steep and, overall, too early in phase to be linked to the previous ones on the basis of the  $f_1=1.02 \text{ d}^{-1}$  term.

The light variation of HR 2740 is too complex to be accounted for by a single  $f_1 = 1.02 \text{ d}^{-1}$  oscillation. Hence, we analyzed the whole set of data; its spectral window shows a higher  $1 \text{ d}^{-1}$  alias, but the frequency resolution is greatly improved by the more extended time baseline (from 9 to 27 days). The upper panel of Fig. 5 reveals the true frequency content. The previously detected peak at  $1.02 \text{ d}^{-1}$  is a blend of two close peaks. In the upper panel the highest peak is at  $1.04 \text{ d}^{-1}$ , and the close peak at  $0.99$  is the highest in the fourth panel. These two terms generated a beat phenomenon. In the JD 2450478–2450487 interval they are in phase coherence, while at the beginning of the observations the shape of the light curve was deformed by the phase oppositions of the two components. In addition, two other terms can be detected, at  $1.10 \text{ d}^{-1}$  (second panel) and around  $0.90$

$\text{d}^{-1}$  (third panel; it is the same term detected in the previous analysis). Since one of them could be the alias of the other ( $0.90=1.00-0.10$ ,  $1.10=1.10+0.10$ ), we checked whether only one of them can explain the light variation by omitting one term in the least-squares solution or by changing the order of introduction of k.c. in the frequency analysis; we always found both in the power spectra. The interaction of one term with the alias of the other enhanced the power of the peak at  $1.10 \text{ d}^{-1}$ , which is detected as the second term even if its amplitude is smaller than that of the  $0.99 \text{ d}^{-1}$  term. We also verified our solution by introducing  $f=1.0434 \text{ d}^{-1}$  and  $f=0.9951 \text{ d}^{-1}$  as k.c., but again the least-squares method found  $f=1.108 \text{ d}^{-1}$  as third component and  $f=0.908 \text{ d}^{-1}$  as the fourth.

When introducing these four frequencies as k.c., we obtained a rather flat spectrum also in the low frequency region (lower panel). If other small amplitude terms are present, they have an amplitude lower than 1 mmag and cannot be detected in a reliable way. We also investigated the possibility that the signal has a non-sinusoidal shape by fitting the sum of a fundamental frequency and several harmonics. Such a procedure give a best-fit frequency of  $1.02 \text{ d}^{-1}$ .

However, the residuals are not white and the removal of several further sinusoids is necessary before the spectrum is as flat as in the bottom panel of Fig. 5, clearly supporting a multiperiodic content.

The presence of a term very close to  $1 \text{ d}^{-1}$  can be considered as suspect, and is possibly due to a misalignment between the two datasets. Firstly, it must be noted that a term close to  $1.04 \text{ d}^{-1}$  is necessary to explain the beating in the light curve. In any case, the most direct way to check its physical nature is to process the dataset comprising the SAAO measurements only. This dataset is affected by the strength of the alias at  $\pm 1 \text{ d}^{-1}$ , but spanning the whole length of the campaign it is adequate to resolve the two peaks, a possibility that the shorter ESO dataset does not offer. Its analysis reveals that, even if the alias at  $2.04 \text{ d}^{-1}$  is as high as the term at  $1.04 \text{ d}^{-1}$  and the  $1.10 \text{ d}^{-1}$  term diverts power to the  $0.90 \text{ d}^{-1}$  one, the term at  $0.99 \text{ d}^{-1}$  is visible in the power spectrum. It is important to note that the analysis of a subset yields us the same frequencies as the whole set; this supports the working idea that the four terms are really present in the light curve and are not generated by one or two terms showing amplitude and/or phase variations, since in such a case the frequency content should change when reducing the sample.

Moreover, we performed additional tests changing the value of the correction in magnitude applied to the SAAO measurements; in all the cases the signal at  $0.99 \text{ d}^{-1}$  is always present. We also noted that the rms residual has the minimum value for the adopted shift (13 mmag), which was calculated from overlapping segments of the light curves and hence is independent of the solution. Moreover, once the accepted solution was obtained, we performed several fits on the two datasets keeping locked some of the parameters and evaluating the differences between the zeropoints. We always obtained a value around 13 mmag, never reaching the 17 mmag value yielded by the average method. Even if the adoption of such an extreme value did not prejudice the determination of the solution, it should be regarded as an artifact of the odd distribution in phase. When considering the discrepancy between the two shifts calculated in the OU Pup case (see Sect. 2.2), we obtain a serious warning against the use of the mean level subtraction as a method to correct systematic shifts.

Hence, we can be very confident of the physical nature of the  $0.99 \text{ d}^{-1}$  term. It must be noted that its amplitude is very similar in  $b$  and  $y$  light, while in the other cases the  $y$  amplitude is about 20% smaller than the  $b$  amplitude. Even if error bars on the amplitudes can account for this discrepancy, it is possible that this term has a geometrical origin, e.g. an ellipsoidicity effect due to a close companion.

Table 3 lists the coefficients of the least-squares fit. Note that in the  $b - y$  data only the  $f_1 = 1.04 \text{ d}^{-1}$  term was considered. Of course, the other terms are present in the  $b - y$  light curve since their amplitudes in  $b$  and  $y$  are different, but since the amplitude differences are less than 1 mmag their consideration changes the rms of the residuals marginally and their least-squares parameters are not useful, being affected by large uncertainties. Unfortunately, since  $u$  and  $v$  measurements were performed at ESO only, the related datasets did not have the necessary resolution to yield a reliable solution which separates the contributions of the two close terms at  $1.04$  and  $0.99 \text{ d}^{-1}$ .

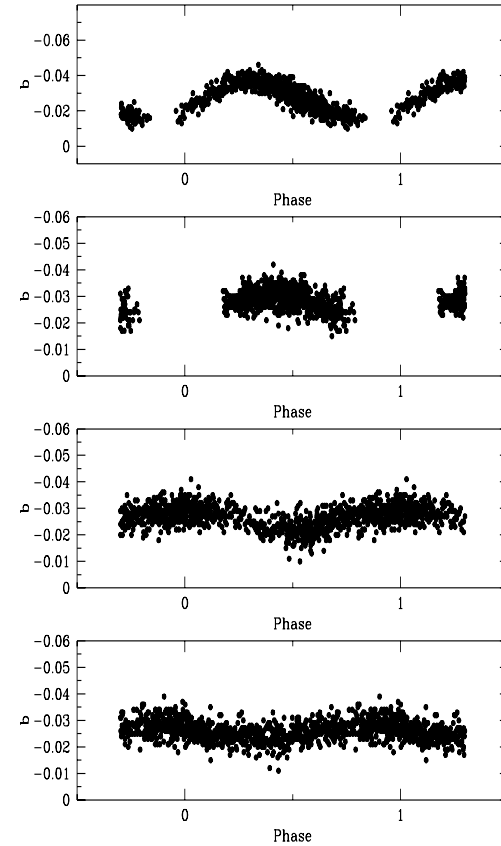


**Figure 6.**  $b$  light curves of the four terms evidenced in the light curve of HR 2740

We also analyzed the time series by means of the CLEAN technique (Roberts et al. 1987), but, as already noted in the case of HD 224845 (Mantegazza et al. 1994), this method is not suitable for frequencies near  $1 \text{ d}^{-1}$  since the subtraction of the average before computing the periodogram removes not only the power at zero frequency, but also most of it at its strong aliases ( $1.0 \text{ d}^{-1}$ ,  $2.0 \text{ d}^{-1}$ , ...).

## 5 DISCUSSION

We established that HR 2740 is a new  $\gamma$  Dor variable, showing a dominant frequency of  $1.043 \text{ d}^{-1}$ , beating with a term at  $0.995 \text{ d}^{-1}$ ; two other terms at  $0.902$  and  $1.109 \text{ d}^{-1}$  complete the fit of the light curve and no other periodicities could be found in our double-site measurements. Figure 6 shows the  $b$  light curves of the four components we identified. To obtain each of them we subtracted the theoretical contribution (by using the least-squares fit listed in Tab. 3) of the other three from the original measurements. To search for possible long-term variations in the frequency content of the oscillations we re-examined the photometric data of Hensberge et al. (1981), where HR 2740 was used as a comparison star. Unfortunately, those measurements are too scanty (21 points on 16 nights spanning 41 days) to provide an additional dataset and to yield details of long-term behaviour.

**Table 3.** Least-squares fit of the data on HR 2740

Freq. [ $d^{-1}$ ]	blue		yellow		$b - y$	
	Ampl. [mmag]	Phase [rad]	Ampl. [mmag]	Phase [rad]	Ampl. [mmag]	Phase [rad]
1.0434	10.5	1.18	8.3	1.23	1.6	1.22
$\pm 0.0004$	$\pm 0.4$	$\pm 0.05$	$\pm 0.3$	$\pm 0.07$	$\pm 0.2$	$\pm 0.23$
0.9951	4.8	0.59	4.6	0.55		
$\pm 0.0010$	$\pm 0.5$	$\pm 0.11$	$\pm 0.5$	$\pm 0.12$		
1.1088	3.5	3.16	2.8	3.28		
$\pm 0.0017$	$\pm 0.2$	$\pm 0.20$	$\pm 0.2$	$\pm 0.24$		
0.9019	2.4	4.14	1.9	4.17		
$\pm 0.0020$	$\pm 0.3$	$\pm 0.15$	$\pm 0.3$	$\pm 0.20$		
$T_0 = \text{Hel. J.D. } 2450463.0000$						
$b_0 = -0.0258 \pm 0.0003$						
Residual rms 3.2 mmag						
878 measurements						
$y_0 = -0.2739 \pm 0.0002$						
Residual rms 3.2 mmag						
878 measurements						
Residual rms 3.7 mmag						
874 measurements						

**Table 4.**  $\gamma$  Dor stars ordered for increasing  $b - y$ : physical parameters obtained from  $uvby\beta$  photometry

Star	$b - y$	$m_1$	$c_1$	$\beta$	$\delta m_0$	$M_V$	$R/R_\odot$	$T_{\text{eff}}$ [ K ]	$\log g$
HR 8799	0.181	0.142	0.678	2.745	0.04	2.85	1.48	7250	4.3
HD 224945	0.192	0.147	0.719	2.743	0.04	2.45	1.82	7200	4.1
HD 224638	0.198	0.154	0.690	2.726	0.02	2.41	1.87	7050	4.0
$\gamma$ Dor	0.206	0.165	0.670	2.742	0.02	2.88	1.52	7200	4.2
9 Aur	0.212	0.155	0.643	2.723	0.02	2.78	1.64	7050	4.2
HR 2740	0.219	0.154	0.640	2.705	0.01	2.44	1.92	6850	3.9
HD 164615	0.230	0.178	0.624	2.715	-0.01	2.80	1.66	7000	4.1
HD 108100	0.234	0.161	0.639	2.705	0.00	2.45	1.97	6850	3.9

### 5.1 Stellar parameters

In recent years, a number of multi-site observing studies have been conducted on this new class of variable stars and it is interesting to compare the new results obtained for HR 2740 with the phenomenology evidenced in previous cases. Reliable  $uvby$  standard photometry is available for HR 2740:  $b - y = 0.219$ ,  $m_1 = 0.154$ ,  $c_1 = 0.640$ ,  $\beta = 2.705$ . By means of the Moon & Dworetsky (1985) calibration we obtained typical values for a star located near the cool border of the classical instability strip, i.e.  $R = 1.92R_\odot$ ,  $T_{\text{eff}} = 6850$  K,  $M_V = 2.44$ ; moreover, the  $\delta m_0$  value of 0.010 suggested normal metal abundances. Curiously, HR 2740 has the same (within the error bars) physical properties of HD 108100; however, this seems true of other  $\gamma$  Dor stars too, as shown by the parameters listed in Tab.4. Since they were obtained by applying the same procedure, the narrow spread of each parameter for different stars has a physical meaning, suggesting us that all the  $\gamma$  Dor stars are very similar objects. The quoted physical parameters can be used to calculate the pulsational constants  $Q_i$  for the four modes observed in the light curve of HR 2740, obtaining  $0.35 < Q_i < 0.43$  d, i.e. values typical for gravity modes. The radial fundamental mode is expected to have a value of about 12  $d^{-1}$ ; no term having an amplitude higher than 1 mmag is found in that region.

### 5.2 Frequency and amplitude values

There are two stars showing a frequency content clustering around a mean value, i.e. HD 108100 (1.32 and 1.40  $d^{-1}$ ) and  $\gamma$  Dor itself (1.32, 1.36 and 1.48  $d^{-1}$ ); on the other hand, HD 224945 and 9 Aur have at least one term largely separated by the others. HR 2740 is very similar to the former stars, since there is no indication of the presence of a term outside the interval 0.90–1.10  $d^{-1}$ . However, the amplitudes are smaller than in the cases of 9 Aur and HD 108100; moreover in HR 2740 there is a dominant term (1.04  $d^{-1}$ ), while in those cases the amplitudes are very similar. Hence, it is not possible to establish common properties in the light curves of  $\gamma$  Dor stars considering only frequency and amplitude values.

Zerbi et al. (1997a; 1997b) emphasized the lack of amplitude in the  $y$  light curve of 9 Aur and HD 164615 when comparing, on the basis of theoretical models, the temperature ranges as determined from the different curves  $y, m_1, c_1, \beta$ . This result finds a partial confirmation in the high  $A_v/A_y$  ratio announced by Breger et al. (1997) on the second frequency of HD 101800 (the same ratio for the first frequency agrees with the theoretical model). In the case of  $\gamma$  Dor itself, the mean  $A_b/A_y$  ratio is around 1.20, for 9 Aur around 1.25, for HD 164615 around 1.30. In the case of HR 2740, the  $A_b/A_y$  ratio is around 1.26 for the  $f_1, f_3, f_4$ . Theoretical models of non-radial  $p$  modes predict an  $A_b/A_y$  ratio in the interval 1.20–1.30 (see, for example, Garrido et

al. 1990). The theoretical model of a  $g$ -mode pulsator proposed by Breger et al. (1997) does not change appreciably the mean value of the  $A_v/A_y$  ratio. Hence to establish how much the observed quantities deviate from theoretical predictions needs a more detailed investigation.

As noted above, the  $f_2$  term yields an  $A_b/A_y$  ratio close to 1.0, which can be explained by uncertainties on the zero-point shifts, rather than by a geometrical effect or by a surplus of  $y$  amplitude. Unfortunately, as often happens in the case of small amplitude variables, the formal error bars reported in Tab. 3 precluded meaningful evaluations of the phase shifts, which could supply some hints about mode identifications.

### 5.3 Light curve stability

The multiperiodicity of  $\gamma$  Dor stars is a well established fact on the basis of the long term survey of  $\gamma$  Dor itself and the results of the recent multisite campaigns on 9 Aur and HD 224945. In those stars, after the subtraction of all known frequencies, the power spectra of the residuals often show a residual unexplained signal and a non-uniform distribution of the noise around the mean light curve. In such a scenario, the small amplitude variable HR 2740 is an exception, since the residual power spectrum is flat (Fig. 5, bottom panel), the fit of the light curve quite good (Fig. 4) and the scatter around the mean light curves is uniform (Fig. 6), not supporting the possibility of a possible change in the maximum brightness from one cycle to the next.

### 5.4 The rotational modulation

In many previous papers it was proposed to explain the complicated light curve observed for the  $\gamma$  Dor variables by the sum of one or two close periodicities (eventually shaped as a double or triple wave) related to the rotational period of the star. The successive multisite campaigns provided much clearer power spectra and it was realized that the observed light curves are generated by the sum of a number of independent frequencies. The results obtained on HR 2740 and their comparison with those obtained on OU Pup and PR Pup (two Ap stars, i.e. two rotating variables) described here yield other pieces of evidence against a rotational variability. The light amplitude of HR 2740 (and of the other  $\gamma$  Dor stars) increases from  $y$  to  $v$ , then decreases in  $u$ , as in the case of pulsating stars; in the case of Ap stars the amplitude is by far greater in  $u$  than in other colours. Moreover, the light curves of the Ap stars are monoperiodic and very stable in amplitude, while the  $\gamma$  Dor stars are multiperiodic and often have the appearance of having unstable amplitudes (Zerbi et al. 1997a for the  $0.7679\text{ d}^{-1}$  term in 9 Aur; Poretti et al. 1996 for all the terms in HD 224945). Of course, Ap stars are hotter and maybe the different physical conditions can introduce a completely different behaviour, but it remains hard to explain why no term of the  $\gamma$  Dor light curves shows a flat part, as currently observed in a rotating variable (see Fig. 2).

**Table 5.** The rotational splitting  $|f - f_o|$  (in  $\text{d}^{-1}$ ) calculated for  $\ell=1$  and  $\ell=2$  assuming  $|m|=1$  and  $v \sin i = 40 \text{ km s}^{-1}$  is shown in function of the  $i$  angle (in degrees);  $\Omega$  indicates the corresponding rotational frequency (in  $\text{d}^{-1}$ )

$i$	$v_{eq}$	$\Omega$	$ f - f_o $	
			$\ell=1$	$\ell=2$
10	230	2.37	1.19	1.97
20	117	1.20	0.60	1.00
30	80	0.82	0.41	0.68
40	62	0.64	0.32	0.53
50	52	0.54	0.27	0.45
60	46	0.48	0.24	0.39
70	42	0.44	0.22	0.36
80	40	0.42	0.21	0.35
90	40	0.41	0.21	0.34

### 5.5 The pulsational model

Two attempts were made to yield a physical explanation of the observed frequencies, interpreted as different pulsation modes. Aerts & Krisciunas (1996) discussed in detail the case of 9 Aur, demonstrating that the rotational splitting can reasonably explain the observed two frequencies (the third one was not known at that time); Breger et al. (1997) proposed a model of HD 108100 based on high-order, independent  $g$ -modes, without considering the effects of the rotation. We performed some calculations using the procedure described by Aerts & Krisciunas (1996), demonstrating that in the case of HR 2740 it is hard to explain the observed frequency separation ( $<0.20 \text{ d}^{-1}$ ) by the splitting of different  $m$  modes. Table 5 reports the expected separation  $|f - f_o|$  for  $\ell=1$  and  $\ell=2$ , assuming a first-order approximation, a  $v \sin i = 40 \text{ km s}^{-1}$  (Slettebak et al. 1975) and  $R = 1.92 R_\odot$ . As can be noted, the frequency spacing increases with  $\ell$  and decreases with  $i$ , admitting a separation of about  $0.20 \text{ d}^{-1}$  only in the limiting case  $\ell=1$  and  $i > 70^\circ$ . However, since most the observed terms have a smaller separation, the rotational splitting does not appear suitable to match the observed frequency spectra of HR 2740; this is also true considering the second order term since the  $\Omega^2/f_o$  correction is marginal for  $\Omega < 0.5 \text{ d}^{-1}$  and  $f_o \sim 1 \text{ d}^{-1}$ ). Of course, this result should be considered with caution, mindful of the warnings by Aerts & Krisciunas (1996) about the application of theoretical models of rotating  $g$ -mode pulsators. The pulsation frequency spectrum of HR 2740 is reminiscent of the very rich frequency spectra of  $\delta$  Sct stars, where a large number of independent frequencies were discovered by performing accurate multisite campaigns (see for example the case of FG Vir, Breger 1995). These campaigns gradually allowed asteroseismological models of the  $\delta$  Sct stars to be proposed. Perhaps this too can be the future of the rapidly developing field of  $\gamma$  Dor stars.

### ACKNOWLEDGEMENTS

D. de Alwis gratefully acknowledges the financial support of Dr. Arthur C. Clarke and the South African Astronomical Observatory which enabled her attendance at the 1997 SAAO Summer School. She further thanks the Director

of the Arthur C. Clarke Centre for Modern Technologies for leave of absence during January 1997. P. Martinez and C. Koen acknowledge the technical support rendered by the SAAO workshops during these observations. E. Poretti thanks the ESO technical staff for the collaboration during the observations; this project is one of the last carried out with the ESO 50-cm telescope before its closing (1997 April 1).

## REFERENCES

Aerts C., Krisciunas K., 1996, MNRAS 278, 877  
 Balona L.A., Krisciunas K., Cousins A.W.J., 1994, MNRAS 270, 905  
 Breger M., 1995, Delta Scuti Star Newsletter 9, 14  
 Breger M., Handler G., Garrido R. et al., 1997, A&A, in press  
 Catalano F.A., Leone F., 1993, A&AS 97, 501  
 Garrido R., Garcia-Lobo E., Rodriguez E., 1990, A&A 234, 262  
 Heck A., Mathys G., Manfroid J., 1987, A&AS 70, 33  
 Hensberge H., Maitzen H.M., Deridder G., Gerbaldi M., Delmas F., Renson P., Doom C., Weiss W.W., Morguleff N., 1981, A&AS 1981, 151  
 Mantegazza L., Poretti E., Zerbi F., 1994, MNRAS 270, 439  
 Moon T.T., Dworetsky M.M., 1985, MNRAS, 217, 305  
 Poretti E., Akan C., Bossi M., Koen C., Krisciunas K., Rodriguez E., 1996, IAU Symposium 181 "Sounding Solar and Stellar Interiors", Nice, in press  
 Poretti E., Zerbi F.M., 1993, A&A, 268, 369  
 Roberts D.H., Lehar J., Dreher J.W., 1987, AJ, 93, 968  
 Slettebak A., Collins G.W., Boyce P.B., White N.M., Parkinson T.D., 1975, ApJS 29, 137  
 Vanićek P., 1971, Ap&SS, 12, 10  
 Zerbi F.M., Garrido R., Rodriguez E., Krisciunas K., Crowe R.A., Roberts M., Guinan E.F., McCook G.P., Sperauskas J., Griffin R.F., Luedke K.D., 1997a, MNRAS, accepted  
 Zerbi F.M., Rodriguez E., Garrido R., Martin S., Akan C., Luedke K.D., Keskin V., Ibanoglu C., Evren S., Tunca Z., Pekunlu R., Paparo M., Nuspl J., Krisciunas K., Jiang S.Y., 1997b, MNRAS, submitted